

# Stochastic Optimum Energy Management for Advanced Transportation Network

Seyed Amin Sajadi-Alamdari\* Holger Voos\*  
Mohamed Darouach\*\*

\* *Interdisciplinary Centre for Security, Reliability and Trust (SnT),  
University of Luxembourg, L-1359 Luxembourg, (e-mail: {amin.sajadi,  
holger.voos}@uni.lu)*

\*\* *Centre de Recherche en Automatique de Nancy (CRAN)  
UMR-CNRS 7039, Université de Lorraine, IUT de Longwy, F-54400  
Cosnes et Romain, France (e-mail:  
mohamed.darouach@univ-lorraine.fr)*

---

**Abstract:** Smart and optimal energy consumption in electric vehicles has high potential to improve the limited cruising range on a single battery charge. The proposed concept is a semi-autonomous ecological advanced driver assistance system which predictively plans for a safe and energy-efficient cruising velocity profile autonomously for battery electric vehicles. However, high entropy in transportation network leads to a challenging task to derive a computationally efficient and tractable model to predict the traffic flow. Stochastic optimal control has been developed to systematically find an optimal decision with the aim of performance improvement. However, most of the developed methods are not real-time algorithms. Moreover, they are mainly risk-neutral for safety-critical systems. This paper investigates on the real-time risk-sensitive nonlinear optimal control design subject to safety and ecological constraints. This system improves the efficiency of the transportation network at the microscopic level. Obtained results demonstrate the effectiveness of the proposed method in terms of states regulation and constraints satisfaction.

*Keywords:* Risk Assessment; Stochastic Optimisation; Nonlinear Control; Real-time Automotive Systems; Intelligent Driver Aids

---

## 1. INTRODUCTION

One of the most promising powertrain technology for the predictable future transportations is provided by Battery Electric Vehicle (BEV). However, the BEVs suffers from limited cruising range also known as *range-anxiety* due to limited onboard energy capacity. Several methods have been developed to extend the cruising range such as the Ecological (Eco) driving concept which refers to a smarter and more energy-efficient anticipated driving style. Ecological Advanced Driver Assistance Systems (Eco-ADAS) can assist human drivers to improve the trip safety and energy-efficiency. For the Eco-ADAS control systems, Model Predictive Control (MPC), also known as receding horizon optimal control, has been an attractive approach. In MPC, an Optimal Control Problem (OCP) is solved repeatedly in a receding horizon principle and the first element in a sequence of finite control actions is applied to the system at each sampling time.

The well-established Adaptive Cruise Control (ACC) and Cooperative Adaptive Cruise Control (CACC) as ADAS have high potential to influence on traffic flow. The ACC and CACC automate the throttle and brake control of

the vehicle to retain the pre-set longitudinal velocity while maintaining a safe distance from preceding vehicles. Several works of literature may be founded. For instance, an energy-efficient linear MPC that use the energy consumption map of a BEV was established by Schwickart et al. (2015a) and Schwickart et al. (2015b). In order to improve the performance specifications of linear MPC, Nonlinear MPC (NMPC) is distinguished by the use of nonlinear system model in the OCP. An instance work of energy-efficient NMPC was introduced by Kamal et al. (2013). Exogenous disturbances and parametric uncertainties are pervasive features of the Eco-ADAS systems. Stochastic MPC (SMPC) has been introduced to handle the system uncertainties and systematically find an optimal decision. The SMPC is based on the stochastic uncertainty of process model and the OCP is mainly formulated as the expectation of objective function with probabilistic constraints, so-called *chance-constraints*. Considering the ACC systems, a scenario-based SMPC with driver behaviour learning capability for improving the performance of powertrain was designed by Bichi et al. (2010). A fast Stochastic NMPC (SNMPC) that extend the functionalities of the ACC system was introduced by Sajadi-Alamdari et al. (2017a). The SNMPC are mainly risk-neutral for safety-critical systems. A risk-averse SNMPC for the extended ACC system has been introduced by Sajadi-Alamdari et al. (2017b).

---

\* This research was supported by FNR "Fonds national de la Recherche" (Luxembourg) through AFR "Aides à la Formation-Recherche" Ph.D. grant scheme No. 7041503.

Although the conventional ACC and CACC systems can assist the human driver to have a safe driving experience, these systems are not capable of dealing with curvy roads and dynamic traffic information in an energy-efficient manner where the driver intervention is required. From control algorithm point of view, most of the mentioned SNMPC are based on risk-neutral performance measures where may not be a suitable strategy for the safety-critical ACC and CACC systems. While Risk-averse SNMPC has shown promise to balance conservatism in decision-making with robustness to uncertainties in a real-time manner, there is an implicit risk at the cost function that is not available in the future prediction, and this risk increases within long-term prediction time-horizon. For this reason, a sophisticated safe and energy-efficient ACC system with extended functionalities that operate in a stochastic traffic environment needs to be explored.

The main contribution of this work is a real-time risk-averse SNMPC (RSNMPC) to enhance the Eco-ACC system for BEVs. The proposed method is substantially different from Sajadi-Alamdari et al. (2017a) and Sajadi-Alamdari et al. (2017b) while deterministic and stochastic components of the system are refined. In this paper, a discount factor is utilised in objective function to associate weights on costs at different stages within the prediction horizon. First, the BEV longitudinal dynamics (host vehicle), its energy consumption, as well as road geometry and traffic sign information are modelled. Second, due to the influence of the preceding vehicle's motion on the energy efficiency of the host vehicle, a physical-statistical dynamic model of the preceding vehicle is adapted. Based on the developed model, a chance-constrained real-time nonlinear receding horizon optimal controller is designed to plan the online cost-effective velocity profile to extend the cruising range. The chance-constraint evaluates the propagated scenario for the relative distance regulation between the preceding and the host vehicles. Then, an Entropic Value-at-Risk (EVAR) as a coherent risk measure is used to quantify the risk involved in constraint violation and rear-end collision by a tightest lower bound. Finally, the performance of the proposed concept is evaluated by simulation tests microscopically in terms of real-time energy-efficient states regulation, and constraints satisfaction.

The remainder of this paper is structured as follows: The system model is introduced in Section 2. The RSNMPC formulation and risk management are presented in Section 3. Section 4 includes simulation evaluation of the proposed concept, followed by the conclusion and future work in Section 5.

### Notation

Throughout this paper,  $\mathbb{R}^n$  denotes the  $n$ -dimensional Euclidean space.  $\mathbb{R}_+ := [0, \infty)$ .  $\mathbb{N} = \{1, 2, \dots\}$  is set of natural numbers.  $\mathbb{N}_+ := \mathbb{N} \cup \{0\}$ .  $\mathbb{Z}_{[a,b]} := \{a, a+1, \dots, b\}$  is set of integers from  $a$  to  $b$ .  $\mathbf{E}$  denotes expectation and  $\mathbf{E}_x[\cdot] := \mathbf{E}[\cdot | x(0) = x]$  is the conditional expectation.  $\mathbf{Pr}$  denotes probability, and  $\mathbf{Pr}_x[\cdot | x(0) = x]$  is the conditional probability distribution of random variable(s)  $x$ .

## 2. SYSTEM MODEL

For the sake of completeness, the Eco-ADAS concept for a semi-autonomous BEV that was introduced by Sajadi-

Alamdari et al. (2017a); Sajadi-Alamdari et al. (2017b) will be reviewed. This concept extends the functionalities of an Eco-ACC system as presented in Fig. 1. Similar to the conventional ACC systems, the driver pre-sets the desired velocity with preferred safe distance from the preceding vehicle. The Semi-autonomous Eco-ACC system predictively regulates the velocity with respect to the longitudinal motion of the host vehicle dynamics (BEV), its energy consumption, road geometric navigation data, traffic sign information, as well as the plausible motion of the preceding vehicle. While the driver handles the steering control of the vehicle, this system should plan a proper safe and energy-efficient cruising velocity profile autonomously for the entire trip without requiring the driver interventions. In addition, this system should be able to handle the cut-in or emergency braking situations.

### 2.1 Vehicle and Energy Dynamics

The position ( $s_h$ ) and velocity ( $v_h$ ) along the longitudinal motion of the BEV (host vehicle) can be expressed by Newton's second law of motion as follows:

$$\dot{s}_h = v_h, \quad (1)$$

$$\dot{v}_h = (F_{trac} - F_{res})/M, \quad (2)$$

where  $M$ ,  $F_{trac}(t)$ , and  $F_{res}(t)$  are equivalent mass of the vehicle, traction force, and total motion resistive forces, respectively (Ehsani et al., 2009). The traction force (throttle and brake pedals) depends on the equivalent mass and control input as  $F_{trac}(t) := Mu(t)$  where the control input is bounded (Sajadi-Alamdari et al., 2016). The main total resistive force including aerodynamic drag, gradient, and rolling resistance forces represented by:

$$F_{res} = \frac{1}{2} \rho A_f C_D (d) v_h^2 + Mg \sin(\theta(s_h)) + C_{rr}(v_h) Mg \cos(\theta(s_h)), \quad (3)$$

where  $\rho$ ,  $A_f$ ,  $g$ ,  $\theta(s_h)$ ,  $C_D(d)$ , and  $C_{rr}(v_h)$ , are the air density, the vehicle frontal area, the gravitational acceleration, the road slope angle as a function of the host vehicle position, aerodynamic drag coefficient as a function of relative distance between the preceding and host vehicles,  $d := s_p - s_h$ , and the velocity dependent rolling resistance coefficient, subsequently (Sajadi-Alamdari et al., 2017b).

For a given velocity at a given traction force, the operating point of the electric machine and the related power consumption or regeneration could be determined (Sajadi-Alamdari et al., 2016). A relation of the traction power-to-mass ratio can describe the energy consumption of the BEV as:

$$\dot{e}_h = f_a (p_{trac}/M) + f_{cruise}, \quad (4)$$

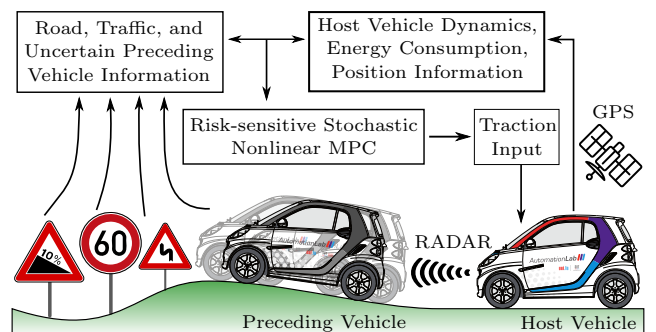


Fig. 1: Extended Eco-ACC System for BEV

where  $p_{trac}$  denotes the traction power,  $f_a := a_2 u^2 + a_1 u + a_0$ , and  $f_{cruise} := b_3 v_h^3 + b_2 v_h^2 + b_1 v_h + b_0$ . This model is capable of capturing the full-range energy consumption of a BEV based on the velocity and the control input. For more details see e.g. (Sajadi-Alamdari et al., 2017a).

## 2.2 Road Geometry and Traffic Model

The road slopes, road curves, and traffic speed limit zone data are modelled as continuous and differentiable functions in (Sajadi-Alamdari et al., 2016). In that method, the road slope profile,  $f_{slp}(\theta(s))$ , is proposed to be the sum of quadratic functions of the position representing each road segments slope data as follows:

$$f_{slp}(\theta(s)) := \sum_{n=1}^{N_{sgm}} H_{(s-s_{n-1})}^n (a_n s^2 + b_n s + c_n) H_{(s-s_n)}^n, \quad (5)$$

where  $N_{sgm}$  is the number of road segments,  $H_{(s-s_{n-1})}^n$  and  $H_{(s-s_n)}^n$  are hyper-functions of the  $n^{th}$  road segment. The simple curve is used to express the total absolute road curve profile,  $f_{crv}(\delta(s))$ , which is defined as:

$$f_{crv}(\delta(s)) := \sum_{n=1}^{N_{crv}} H_{(s-s_{ent})}^n \left| \frac{1}{R_{crv_n}(s)} \right| H_{(s-s_{ext})}^n, \quad (6)$$

where  $N_{crv}$  is the number of road curves, and  $R_{crv_n}$  is the radius of a circle valid for the curve's arc length with two position points,  $s_{ent}$  and  $s_{ext}$ , at the respective entrance and exit position. Furthermore, the traffic speed limit profile,  $f_{lmt}(s)$ , can be modelled as:

$$f_{lmt}(s) := \sum_{n=1}^{N_{lmt}} H_{(s-s_{str})}^n (v_{lmt_n} - v_{max}) H_{(s-s_{end})}^n + v_{max}, \quad (7)$$

where  $N_{lmt}$  is the number of speed limit zones, and  $v_{lmt_n}$  is the specified speed limit value at positions starts from  $s_{str}$  up to the end of the zone  $s_{end}$ . The  $v_{max}$  is the maximum speed value of the host vehicle. For more details, see e.g. Sajadi-Alamdari et al. (2016, 2017a).

## 2.3 Preceding Vehicle Physical-Statistical Motion Model

High entropy in traffic system leads to a challenging task to derive a computationally efficient and tractable model to predict plausible traffic flow. A physical-statistical motion model of the preceding vehicle robust to far-term future prediction was developed by Sajadi-Alamdari et al. (2017a); Sajadi-Alamdari et al. (2017b). The proposed model is based on 85<sup>th</sup> percentile speed concept and road geometry information. The 85<sup>th</sup> percentile speed is referred to *spot speed study*, defined as the speed at or below which 85<sup>th</sup> percent of vehicles travel a given location based on free-flowing conditions over a time period. In addition, other factors such as road slope profile, and traffic speed limit zones information can be considered to estimate a more appropriate velocity trajectory as follows:

$$\dot{s}_p := v_p, \quad (8)$$

$$\dot{v}_p := X_{85^{th}} \left( 1 - \left( \frac{v_p}{f_{85^{th}}} \right)^4 - \frac{\sin(f_{slp}(\theta(s_p)))}{\sin(\frac{\pi}{4})} \right), \quad (9)$$

$$f_{85^{th}} := \min\{\omega_{85^{th}} v_{85^{th}}(f_{crv}(\delta(s_p))), f_{lmt}(s_p)\}, \quad (10)$$

$$v_{85^{th}}(\delta(s_p)) := m_1 \exp(-m_2 \delta(s_p)) + m_3 \exp(-m_4 \delta(s_p)), \quad (11)$$

where  $X_{85^{th}}$  is the acceleration of the preceding vehicle. The position based function  $v_{85^{th}}(\cdot)$ , represents the 85<sup>th</sup> percentile curve speed of the vehicles along the road curves. For more details, see Sajadi-Alamdari et al. (2017a); Sajadi-Alamdari et al. (2017b). To conclude, the introduced model is continuous and differentiable, which is capable of propagating a plausible trajectory for the preceding vehicle motion along the prediction horizon.

## 3. OPTIMAL CONTROL & RISK MANAGEMENT

In the interest of completeness, a general SNMPC formulation and Entropic Value-at-Risk as a coherent risk measure will be reviewed. Afterwards, the proposed risk-averse certainty equivalent reformulation of the RSNMPC and its application for the Eco-ACC system will be presented.

### 3.1 Stochastic Nonlinear Model Predictive Control

Consider a general stochastic, discrete-time system:

$$x_{t+1} = f(x_t, u_t, \omega_t), \quad (12)$$

where  $t \in \mathbb{N}_+$ ;  $x_t \in \mathbb{R}^{n_x}$  is the system states vector;  $u_t \in \mathbb{U} \subset \mathbb{R}^{n_u}$  is a non-empty measurable set for the inputs, and  $\omega_t \in \mathbb{R}^{n_\omega}$  is disturbances vector that is unknown at the current and future time instants. The  $\omega_t$  is composed of i.i.d. random variables within the known sample space  $\Omega$ , the set of events ( $\sigma$ -algebra)  $\mathcal{F}$ , and the allocations of probabilities,  $\mathcal{P}$  to events (exogenous information). The  $f(\cdot)$  is nonlinear Borel-measurable vector of functions that describes the system dynamics (Mesbah, 2016).

Let  $N \in \mathbb{N}$  be the both state and control prediction horizon. Define an  $N$ -stage feedback control policy as:

$$\boldsymbol{\pi} := \{\pi_0(\cdot), \pi_1(\cdot), \dots, \pi_{N-1}(\cdot)\}, \quad (13)$$

where the Borel-measurable function  $\pi_i(\cdot) : \mathbb{R}^{(i+1)n_x} \rightarrow \mathbb{U}$ , for all  $i = 0, \dots, N-1$  is a general state feedback control law (Mesbah, 2016). The control input  $u_i$  is selected as the feedback control law  $u_i = \pi_i(\cdot)$  at the  $i^{th}$  stage of the control policy. In receding horizon optimal control, the cost function of the OCP is commonly defined as:

$$V_N(x_t, \boldsymbol{\pi}) := \mathbf{E}_{x_t} \left[ \sum_{i=0}^{N-1} J_c(\hat{x}_i, u_i) + J_f(\hat{x}_N) \right], \quad (14)$$

where  $J_c : \mathbb{R}^{n_x} \times \mathbb{U} \rightarrow \mathbb{R}_+$  and  $J_f : \mathbb{R}^{n_x} \rightarrow \mathbb{R}_+$  are the *cost-per-stage function* and the *final cost function*, respectively, and  $\hat{x}_i$  denotes the predicted states at time  $i$  given the initial states  $\hat{x}_0 = x_t$ , control law  $\{\pi_i(\cdot)\}_{i=0}^{i-1}$ , and disturbance realizations  $\{\omega_i\}_{i=0}^{i-1}$  (Mesbah, 2016).

A general form of individual chance-constraints is defined by:

$$\Pr_{x_t} [g_j(\hat{x}_i) \leq 0] \geq \beta_j, \quad \text{for all } j = 1, \dots, s, i = 1, \dots, N, \quad (15)$$

where  $g_j : \mathbb{R}^{n_x} \rightarrow \mathbb{R}$  is a Borel-measurable function,  $s$  is the total number of inequality constraints, and  $\beta_j \in (0, 1]$  denotes the lower bound for the probability of  $g_j(\hat{x}_i) \leq 0$  that need to be satisfied.

Using the cost function (14) and the individual chance-constraint (15), the stochastic OCP for (12) is formulated as follows (Mesbah, 2016):

$$V_N^*(x_t) := \underset{\pi}{\text{minimise}} \quad V_N(x_t, \pi) \quad (16a)$$

subject to:

$$\hat{x}_{i+1} = f(\hat{x}_i, \pi_i, \omega_i), \quad \text{for all } i \in \mathbb{Z}_{[0, N-1]}, \quad (16b)$$

$$\pi_i(\cdot) \in U, \quad \text{for all } i \in \mathbb{Z}_{[0, N-1]}, \quad (16c)$$

$$\Pr_{x_t}[g_j(\hat{x}_i) \leq 0] \geq \beta_j, \quad \text{for all } j \in \mathbb{Z}_{[1, s]}, i \in \mathbb{Z}_{[1, N]}, \quad (16d)$$

$$\omega_i = (\Omega, \mathcal{F}, \mathcal{P}), \quad \text{for all } i \in \mathbb{Z}_{[0, N-1]}, \quad (16e)$$

$$\hat{x}_0 = x_t, \quad (16f)$$

where  $V_N^*(x_t)$  denotes the optimal value function under the optimal control policy  $\pi^*$ . The stochastic OCP in receding horizon principle involves applying the first element of the control action sequence  $u_t = \pi_0^*(\cdot)$  repeatedly to the system at each time instance.

Finding a solution for the stochastic OCP (16) that is ideal for all possible scenarios is a challenging task for real-time safety-critical nonlinear systems. Generally one may replace uncertainties with samples that can be represented as scenarios. In this method  $\hat{\omega}_i$  interpreted as the prediction of expected disturbance values,  $\hat{\omega}_i = \mathbf{E}[\omega_i]$ , for the uncertainty propagation. Consequently, the system function (12) can be rewritten as deterministic surrogate form as:

$$\bar{x}_{t+1} = \bar{f}(\bar{x}_t, u_t), \quad (17)$$

where  $\hat{x}_t \in \mathbb{R}^{n_x + n_\omega}$  denotes the predicted nominal states including auxiliary states  $\hat{\omega}_i$ . The i.i.d random variables assumption of the  $\omega_i$  is no longer required. Therefore, the stochastic OCP cost function defined by (14) reduces to certainty equivalent form. However, it is resealable to assume that the predicted cost for long-term or infinite-time future prediction horizon is less costly in compare to near-term future prediction horizon. Thus, the deterministic certainty equivalent cost function can be accomplished through the parameter  $\rho$  known as *discount factor* which reduce the future cost to the present cost value. In this paper we investigate a certainty equivalent cost function with continuous discount factor on a long  $T$  or infinite horizon OCP as follows:

$$V_T(\bar{x}(t), \pi) := \int_t^{t+T} \exp^{-\rho t} J_c(\bar{x}(t), u(t)) dt, \quad (18)$$

where  $\rho \in [0, 1)$  is discount factor and the cost-per-stage is  $J_c : \mathbb{R}^{n_x + n_\omega} \times \mathbb{U} \rightarrow \mathbb{R}_+$ . This also is referred as current-value Hamiltonian which mainly arises in economic growth theory. It is common to use indirect methods of optimal control to derive the First-order Necessary Condition of Optimality and a Two-Point Boundary-Value Problem has to be solved. It is noteworthy that  $J_f(\hat{x}(t_f)) = 0$  which is know as standard *transversality* conditions. For more information see e.g., Würth et al. (2009); Ohtsuka (2004).

### 3.2 Entropic Value-at-Risk

The Value-at-Risk (VaR) and Conditional VaR (CVaR) are the most popular and widely used risk measurements. A coherent risk measure satisfies the *transitional invariance*, *sub-additivity*, *monotonicity*, and *positive homogeneity* properties. The VaR and CVaR intuitively evaluate the expectation and conditional expectation of (15) respectively on a tail part of its distribution ( $\beta_j$ -percentile). However, the VaR does not satisfy the sub-additivity property while CVaR cannot be computed efficiently. In order to address these limitations, the coherent Entropic VaR

(EVaR) has been recently introduced by Ahmadi-Javid (2012). The EVaR provides the tightest upper bound one can find using the Chernoff inequality for the VaR and CVaR with the same confidence levels. The EVaR with confident level ( $\beta_j = 1 - \alpha_j$ ) is defined as follows:

$$EVaR_{1-\alpha_j}(g_j(\hat{x}_i)) := \inf_{z > 0} \{z^{-1} \ln(M_{g_j(\hat{x}_i)}(z)/\alpha_j)\}, \quad (19)$$

where  $M_{g_j(\hat{x}_i)} = \mathbf{E}_{x_t}[\exp(zg_j(\hat{x}_i))]$  is the moment-generating function of  $g_j(\hat{x}_i)$ . The properties of coherent risk measure have intuitive interpretations in the financial industry, which can be extended to energy management systems. In the case of Extended Eco-ACC system, for instance, the relative distance can be interpreted as a portfolio of energy consumption and travel time. In this paper, we minimise the OCP given by (16) with updated cost function (18) based on coherent risk measure EVaR (19) to handle the chance constraints.

### 3.3 Case Study: Extended Eco-ACC System

The state vector for the Extended Eco-ACC system is defined as  $x_t = [s_h, v_h, e_h]^T \in \mathbb{R}^3$ ; the control input is the traction input applied on host vehicle as  $u_t = u \in \mathbb{U} \subset \mathbb{R}$ ; the measurable disturbance (e.g., Radar-based system) defined as  $\omega_{t-1} = [s_p, v_p]^T \in \mathbb{R}^2$ . We replace the disturbances as auxiliary states concatenated with system state vector as nominal state vector. From Eqs. (1), (2), (4), (8), and (9), the extended state vector is:  $\bar{x}_t = [\dot{s}_h, \dot{v}_h, \dot{e}_h, \dot{s}_p, \dot{v}_p]^T$ .

The cost-per-stage function for Extended Eco-ACC system is defined as:

$$V_N(x_t, \pi) := \sum_{i=0}^{N-1} (1 - \rho)^i (\|\hat{x}_i - x_{ref}\|_Q^2 + \|u_i - u_{ref}\|_R^2), \quad (20)$$

where  $Q, R$  are corresponding weights. The  $u_{ref} = F_{ref}/M$  and the control input defined as a hard box constraint as follows:

$$u_{min}(v_h) \leq u(t) \leq u_{max}(v_h). \quad (21)$$

The following state constraints are implemented as soft constraints. The lateral acceleration of the host vehicle ( $\psi_t$ ) should be lower than the comfort level ( $\psi_{ref}$ ) almost surely ( $\beta_1 = 1$ ) as follows:

$$\Pr_{\psi_t}[g_1(\hat{s}_{h_i}, \hat{v}_{h_i}) := \hat{v}_{h_i}^2 / f_{crv}(\delta(\hat{s}_{h_i})) \leq \psi_{ref}] \geq \beta_1. \quad (22)$$

The velocity of the host vehicle almost surely ( $\beta_2 = 1$ ) should also be lower than speed limit zones as:

$$\Pr_{s_t}[g_2(\hat{s}_{h_i}, \hat{v}_{h_i}) := \hat{v}_{h_i} \leq f_{lmt}(\hat{s}_{h_i})] \geq \beta_2. \quad (23)$$

In addition, relative distance should be larger than the spacing policy ( $d_{ref} := d_0 + v_h t_{hw}$ ) (for more detail see e.g., Sajadi-Alamdari et al. (2016)) with  $\beta_3$  confident level:

$$\Pr_{d_i}[g_3(\hat{d}_i) := d_{ref} \leq \hat{d}_i] \geq \beta_3. \quad (24)$$

In addition, the velocity should be within the standstill and the reference set-point almost surely ( $\beta_4 = 1$ ) as follows:

$$\Pr_{v_{h_t}}[g_4(\hat{v}_{h_i}) := 0 \leq \hat{v}_{h_i} \leq v_{h_{ref}}] \geq \beta_4 \quad (25)$$

where  $v_{h_{ref}}$  is the reference set-point. The energy consumption of the BEV should be less than the reference value ( $e_{h_{ref}}$ ) almost surely ( $\beta_5 = 1$ ) as follows:

$$\Pr_{e_{h_t}}[g_5(\hat{e}_{h_i}) := \hat{e}_{h_i} \leq e_{h_{ref}}] \geq \beta_5. \quad (26)$$

#### 4. SYSTEM EVALUATION

The proposed Extended Eco-ACC system has been evaluated with numerical simulations using realistic values of the parameters on a test track. A *Smart Fortwo third generation* commercial BEV, which is available for practical experiments, is chosen here to model the dynamics of a BEV and its energy consumption (Schwickart et al., 2015b; Sajadi-Alamdari et al., 2017b). The prediction horizon for the predictive controller is set to  $T = 10\text{ s}$  with  $N = 20$  discretized steps. The constants in performance index function are set as  $Q = \text{diag}[0, 1, 0, 0, 0]$ ,  $R = \text{diag}[40]$ , the confidence level for the relative distance chance constraint is set to  $\beta_3 = 0.95$  and discount factor is  $\rho = 0.07$ .

In order to compare the mentioned works of literature with the proposed approach in a fair and informative manner, the European Urban Driving Cycle (EUDC) is used to represent the preceding vehicle velocity profile. We have compared the proposed RSNMPC with the SMPC presented by Bichi et al. (2010) and deterministic NMPC (DNMPC) introduced by Kamal et al. (2013) to show the performance enhancements. The cruising velocity reference is fixed to  $v_{h_{ref}} = 26\text{ m/s}$  with the same values for  $d_0 = 4\text{ m}$  and  $t_{hw} = 3\text{ s}$  considered by Bichi et al. (2010). Fig. 2a shows the performance of controllers in terms of velocity regulations. The RSNMPC track the preceding vehicle and cruising reference with less over/under-shoot compared to the SMPC. Fig. 2b shows the relative distance regulation performance. The DNMPC and SMPC hardly satisfy the relative distance constraint with large variance around

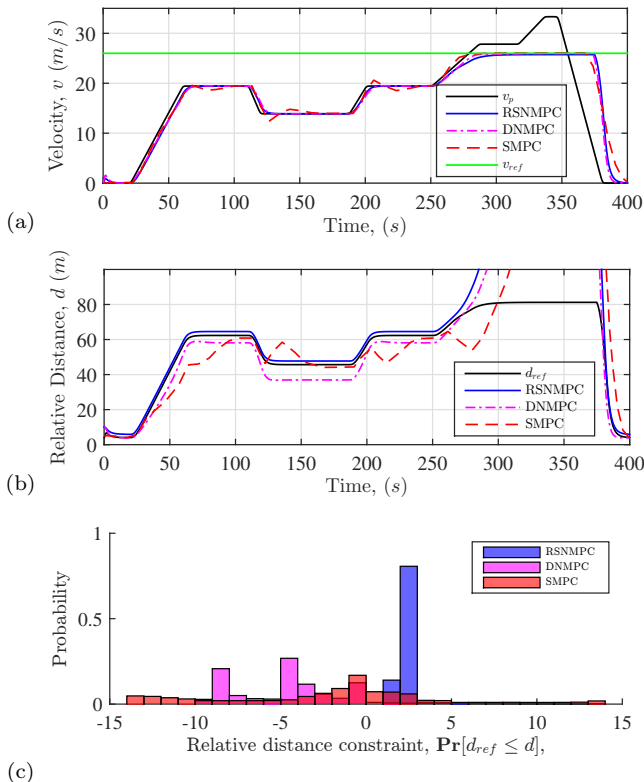


Fig. 2: Performance of controllers for (a) Velocity regulation, and (b) Relative distance regulation, with (c) probability of chance constraint around violation region

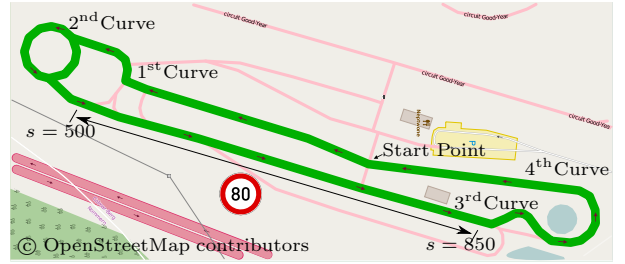


Fig. 3: Test track, Centre de Formation pour Conducteurs

the violation region. On the other hand, the RSNMPC fulfils the chance constraint lower bound requirement with minimum variance. This is shown in Fig. 2c by noting that the positive values are the constraint satisfaction while the negative values represent the constraint violation.

The OCP calculation time for the proposed RSNMPC is around  $5.7\text{ ms}$ , compared to the SMPC with  $1\text{ s}$  and DNMPC with  $2.2\text{ ms}$  on the Intel<sup>®</sup> Core<sup>™</sup> i7 with a memory of  $7.7\text{ GiB}$  PC. The proposed RSNMPC is  $+0.5\%$  more energy efficient than the DNMPC method while respects the OCP constraints satisfaction. In the carried out simulations, the road is assumed to be flat and straight with no speed limit zones. Thus, there are few potentials to save energy which achieved by accounting the energy consumption dynamics. In other words, for longer trips with more hilly and curvy roads, the proposed method has higher potential to save energy.

In addition, performance of the RSNMPC is evaluated on a realistic hilly and curvy roads. A closed test track located at Colmar-Berg in Luxembourg, is chosen to model the road geometry with traffic information (Fig. 3). The test track has a total length of  $1.255\text{ km}$  and includes curves and speed limit zone with relative slope profile (for more detail, see e.g., Sajadi-Alamdari et al. (2016)). Fig. 4a shows the performance of velocity regulations with the RSNMPC in compare to Perfect NMPC (PNMPC), where the uncertainty is exactly known in advance along the prediction horizon. The BEV follows the preceding vehicle with close spacing setting as  $d_0 = 6\text{ m}$  and  $t_{hw} = 1.5\text{ s}$  which could improve traffic flow microscopically.

The controllers speeding up until the BEV reaches the first and second curves ( $20 \leq t \leq 40$ ) where the lateral acceleration constraint should be satisfied. As it is shown, the RSNMPC is faster than the PNMPC controller. However, during the first and second curves, the RSNMPC and PNMPC show similar behaviour. Fig. 4b shows the relative distance regulation performance where the RSNMPC is more conservative than PNMPC in this part of the test track. Afterwards, the controllers increase velocity again up to the point the third and fourth curves are in its prediction horizon ( $83 \leq t \leq 109$ ) where both controllers slow down to fulfil the lateral acceleration constraint on curves. Since the RSNMPC is not aware of the future realised velocity profile of the preceding vehicle, it shows less optimum behaviour in compare to the PNMPC. However, the RSNMPC shows similar behaviour close to the PNMPC performance within  $64 \leq t \leq 114$ . Finally, the controllers speed up once more to reach the starting point while satisfying the relative distance safety constraint.

Fig. 4c shows the performance of the RSNMPC in compare to PNMPC in terms of Inverse of Time To Collision ( $TTC^{-1} := \frac{v_p - v_h}{d}$ ) probability distribution which is a direct and continuous indicator for the collision risk. It is noteworthy that the lower values indicate the more dangerous situations while zero implies the preserving trend. The RSNMPC shows sharp velocity and relative distance regulations which increase its energy consumption. However, due to statistically accurate prediction model of the preceding vehicle and considering the upcoming road geometries with energy consumption map of the *Smart-ED*, the RSNMPC ( $e_h = 0.1844 kW$ ) is +90% as energy-efficient as PNMPC ( $e_h = 0.1671 kW$ ) on the test track despite unknown system uncertainty.

## 5. CONCLUSIONS AND FUTURE RESEARCH

A semi-autonomous ecological advanced driver assistance system which autonomously plans for a safe and energy-efficient cruising velocity profile for the battery electric vehicles was introduced. Real-time risk-averse stochastic nonlinear model predictive control was designed to find the optimal decision with the aim of performance improvement in energy efficiency and constraints satisfaction in a stochastic traffic environment. This system improves the range of electric vehicles and the efficiency of the transportation network at the microscopic level. Obtained results demonstrate the effectiveness of the proposed system compared to the state-of-the-art methods. Further

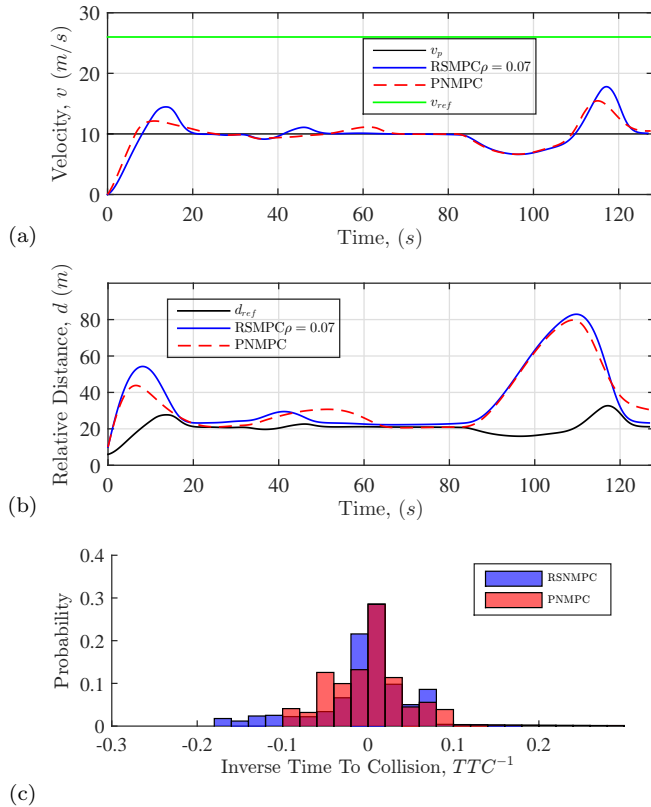


Fig. 4: Performance of RSNMPC vs. PNMPC for (a) Velocity regulation, (b) Relative distance regulation, and (c) Inverse Time To Collision ( $TTC^{-1}$ )

practical experiments will be conducted to validate the introduced concept in more complex scenarios.

## REFERENCES

- Ahmadi-Javid, A. (2012). Entropic Value-at-Risk: A New Coherent Risk Measure. *Journal of Optimization Theory and Applications*, 155(3), 1105–1123. doi:10.1007/s10957-011-9968-2.
- Bichi, M., Ripaccioli, G., Di Cairano, S., Bernardini, D., Bemporad, A., and Kolmanovsky, I. (2010). Stochastic model predictive control with driver behavior learning for improved powertrain control. In *49th IEEE Conference on Decision and Control (CDC)*, 6077–6082. IEEE. doi:10.1109/CDC.2010.5717791.
- Ehsani, M., Gao, Y., and Emadi, A. (2009). *Modern Electric, Hybrid Electric, and Fuel Cell Vehicles: Fundamentals, Theory, and Design*. CRC Press, 2, illustr edition.
- Kamal, M.A.S., Mukai, M., Murata, J., and Kawabe, T. (2013). Model Predictive Control of Vehicles on Urban Roads for Improved Fuel Economy. *IEEE Transactions on Control Systems Technology*, 21(3), 831–841. doi:10.1109/TCST.2012.2198478.
- Mesbah, A. (2016). Stochastic Model Predictive Control: An Overview and Perspectives for Future Research. *IEEE Control Systems*, 36(6), 30–44. doi:10.1109/MCS.2016.2602087.
- Ohtsuka, T. (2004). A continuation/GMRES method for fast computation of nonlinear receding horizon control. *Automatica*, 40(4), 563–574. doi:10.1016/j.automatica.2003.11.005.
- Sajadi-Alamdari, S.A., Voos, H., and Darouach, M. (2016). Nonlinear Model Predictive Extended Eco-Cruise Control for Battery Electric Vehicles. In *24th Mediterranean Conference on Control and Automation (MED)*, 467–472. IEEE, Athens. doi:10.1109/MED.2016.7535929.
- Sajadi-Alamdari, S.A., Voos, H., and Darouach, M. (2017a). Fast stochastic non-linear model predictive control for electric vehicle advanced driver assistance systems. In *IEEE International Conference on Vehicular Electronics and Safety (ICVES)*, 91–96. IEEE. doi:10.1109/ICVES.2017.7991907.
- Schwickart, T., Voos, H., Hadji-Minaglou, J.R., Darouach, M., and Rosich, A. (2015a). Design and simulation of a real-time implementable energy-efficient model-predictive cruise controller for electric vehicles. *Journal of the Franklin Institute*, 352(2), 603–625. doi:10.1016/j.jfranklin.2014.07.001.
- Schwickart, T., Voos, H., Hadji-Minaglou, J.R., and Darouach, M. (2015b). A Fast Model-Predictive Speed Controller for Minimised Charge Consumption of Electric Vehicles. *Asian Journal of Control*, 18(1), 133–149. doi:10.1002/asjc.1251.
- Sajadi-Alamdari, S.A., Voos, H., and Darouach, M. (2017b). Risk-averse Stochastic Nonlinear Model Predictive Control for Real-time Safety-critical Systems. In *The 20th World Congress of IFAC*, 6165–6171. IFAC, Toulouse, France. doi:10.1016/j.ifacol.2017.08.1431.
- Würth, L., Rawlings, J.B., and Marquardt, W. (2009). Economic Dynamic Real-Time Optimization and Nonlinear Model-Predictive Control on Infinite Horizons. *IFAC Proceedings Volumes*, 42(11), 219–224. doi:10.3182/20090712-4-TR-2008.00033.